# STATUS OF THE ERLP PHOTOINJECTOR DRIVE LASER

L.B. Jones\*, ASTeC – Accelerator Science and Technology Centre, STFC<sup>†</sup> Daresbury Laboratory, Warrington WA4 4AD, United Kingdom

#### Abstract

The Energy Recovery Linac Prototype (ERLP) accelerator under construction at Daresbury Laboratory uses a DC photoinjector gun, identical to the IR–FEL injector [1] at the Thomas Jefferson National Accelerator Facility. The drive laser system was specified by the Central Laser Facility at the Rutherford Laboratory, and was installed at Daresbury in February of 2005. The following report gives an overview of the system, and outlines the experience gathered during its operation for the first months of photoinjector commissioning.

### INJECTOR OVERVIEW

The injector is a DC photocathode gun operating at  $350 \,\mathrm{kV}$ . It utilises a caesiated gallium arsenide (Cs:GaAs) cathode, and is specified to deliver  $80 \,\mathrm{pC}$  per electron bunch. The gun is driven at a maximum duty cycle of 0.2%, representing an average electron beam current of  $13 \,\mu\mathrm{A}$ .

#### LASER SYSTEM

The drive laser is a  $High \, Q$  IC10000 Picotrain model, delivering >10 W at 1064 nm wavelength. The lasing medium is diode-pumped neodymium yttrium vanadate (Nd:YVO<sub>4</sub>). It is mode-locked using a SESAM and generates horizontally-polarised 7 ps FWHM pulses at a repetition rate of 81.25 MHz, this being the  $16^{th}$  subharmonic of the 1.3 GHz RF frequency chosen for the ERLP. The drive laser optical system defines and delivers macrobunches to the cathode at a repetition rate up to 20 Hz. The length of a macrobunch may be from a single laser pulse, up to a  $100 \, \mu s$  pulse train. The layout of components on the optical table is shown in figure 2.

## Macrobunch generation

The  $81.25\,\mathrm{MHz}$  pulse train is first chopped into  $130\,\mu\mathrm{s}$  macrobunches at a  $100\,\mathrm{Hz}$  repetition rate. A shutter following the chopper reduces the repetition rate to 1, 2, 5,  $10\,\mathrm{or}\,20\,\mathrm{Hz}$ . The beam polarisation is then rotated to vertical by a  $\frac{\lambda}{2}$  plate. Finally, a KD\*P (potassium di-hydrogen phosphate) Pockels cell defines the beginning and end of the macrobunch by rotating the polarisation back to horizontal before the beam passes through a polarisation analyser. The slopes on the leading and trailing edges of the macrobunch are removed (these arise as the chopper wheel sweeps across the pulse train), and the macrobunch has well–defined edges. The process is illustrated in figure 1.

## Laser beam processing

Second–harmonic generation (SHG) is carried out after macrobunch generation. The non–linear nature of the SHG process serves to enhance the contrast ratio of the Pockels cell. With the SHG bolted to the front of the laser oscillator, the IC10000 generates 67 nJ per pulse at 532 nm. However, in our configuration, following losses in the macrobunch generation optical elements which precede SHG, there is typically 40 nJ per pulse at 532 nm. A pinhole with  $\sim 70\%$  transmission is located immediately after the SHG unit.

Diagnostics which can be viewed remotely are present for both the 1064 and 532 nm beams, as shown in figure 2. The turning mirrors before and after the SHG unit transmit 1% and 2% of the infrared and green beams respectively. The diagnostic beams then pass through beamsplitters and are used to generate images via screen & camera combinations, and feed photodiodes.

A motorised  $\frac{\lambda}{2}$  plate and polariser serve as a beam attenuator, controlled via an EPICS [2] synoptic. A pulse stretcher comprising two separate YVO<sub>4</sub> crystals can be included in the optical setup. This increases the natural 7 ps FWHM pulse length to either 13 ps if one crystal is used, or 28 ps with both.

2% of the 1064 nm beam emerging from the laser oscillator is preserved and passed into the laser beam transport system (L-BTS) for delivery to the injector in tandem with the high–power 532 nm beam. This is for the purpose of synchronising the laser oscillator with the RF systems, as will be explained shortly.

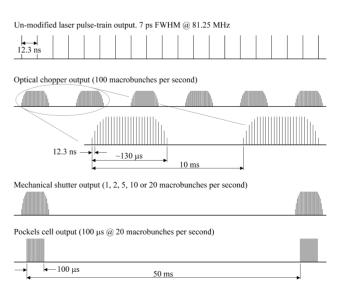


Figure 1: Schematic showing the conversion of the laser oscillator output to the ERLP macrobunch structure.

<sup>\* 1.</sup>b.jones@stfc.ac.uk

<sup>†</sup> Science and Technology Facilities Council

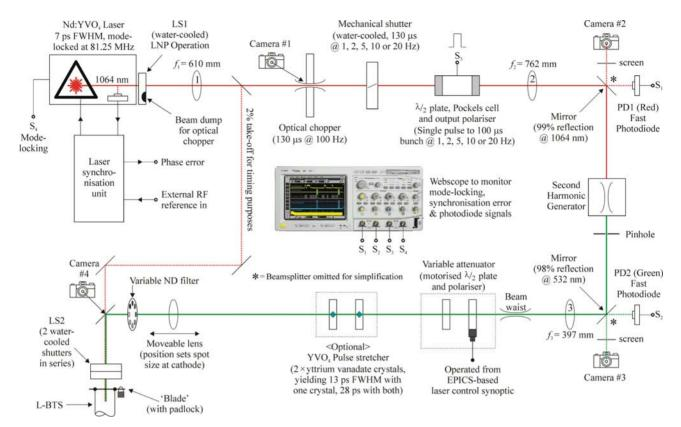


Figure 2: Schematic showing the layout of the optical system for the ERLP photoinjector drive laser.

#### Laser beam transport system (L-BTS)

The L-BTS is comprised of several KF-sealed vacuum vessels and tubes, and incorporates two motorised mirrors which permit the laser beam to move on the cathode surface. The L-BTS for the IR-FEL at Jefferson Laboratory is fixed to the roof of the FEL vault, and vessels containing optical elements have large apertures which can be removed easily for alignment purposes. In contrast, the ERLP L-BTS is fixed to the floor and is partially obscured behind radiation shielding adjacent to the injector. Its vessels do not contain removable apertures, so they must be completely removed to permit alignment of the optical elements. Re-fitting of these vessels inevitably disturbs the alignment of the L-BTS optical elements. With hindsight, either the addition of diagnostic cameras within the L-BTS to monitor beam position on its optics, or the provision of generous apertures in the vessels at the design stage would be highly beneficial. Transmission of the L-BTS has been measured, and found to be  $\sim 70\%$ .

The L-BTS includes a beamsplitter located immediately below the injector which diverts 1% of the 532 nm beam to a CCD camera, positioned such that its detector lies the same distance from the beamsplitter as the cathode surface itself. This is our *virtual cathode*, and it provides an image of the drive laser beam delivered to the actual cathode surface. This is a very useful diagnostic as it includes a cross—hair, and so gives the operator a clear visual indication of relative beam movement on the cathode surface.

### Temperature regulation

The range of temperatures experienced inside the Faraday–shielded laser room and the overhead equipment rack was identified as a problem. A new highly–specified air conditioning system capable of maintaining  $\pm 1\,^{\circ}\text{C}$  in the laser room has been installed recently. Initial results are encouraging, but no data is available yet.

Problems have also been encountered with the laser water cooling circuit. Corrosion within either the laser head or recirculating chiller has led to a continued accumulation of particulate matter. Buildup of this material inside the laser oscillator over time causes a drop in the coolant flow rate, eventually causing shut—down of the pump diode due to over—temperature.

#### Performance of the shutter & Pockels cell

The mechanical shutter (see figure 2) which sets the macrobunch repetition rate has failed twice. It has since been withdrawn by its manufacturer, *nmLaser products*.

Our measurements have shown the benefit of placing the SHG unit after the Pockels cell, but *ringing* of this KD\*P cell has also been observed. This is characteristic of the KD\*P material as both the application and removal of HV to the cell electrodes excites a slow (in comparison to its electrons) oscillation of ions in the crystal lattice. This creates a damped oscillation in the cell's birefringence, manifesting itself as an intensity modulation (*ringing*) in the

transmitted laser beam. The magnitude of the ringing introduced at 1064 nm is then exaggerated by the non–linear SHG process, appearing as a larger ripple at 532 nm.

A Pockels cell which uses RTP (rubydium titanyl phosphate) has been purchased recently, but has not yet been tested. This class of optically-active material has both advantages and disadvantages when utilised in a Pockels cell, in comparison to the more-conventional KD\*P, but it is expected to exhibit considerably less ringing when tested.

#### SYNCHRONISATION AND TIMING

The ERLP drive laser system has been used to further our timing and synchronisation research commitments under the Eurofel DS3 work package. The IC10000 is synchronised to the RF master clock via an external control unit, and uses both motor–driven and piezo–mounted mirrors to actively adjust the laser oscillator cavity length and maintain synchronisation. A HP3047A phase noise analysis system has been used to measure timing jitter between the laser oscillator and the RF master clock.

Closely following techniques published by Scott *et al.* [3], the mixer has been modified to run on battery power. This reduces the noise floor of the measurement system, as shown in figure 3. The effectiveness of various measures to improve synchronisation and reduce jitter have been tested and quantified using the HP3047A, most of which are based on improving isolation of the laser oscillator from acoustic and mechanical noise sources.

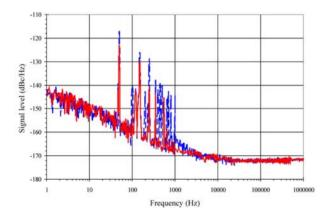


Figure 3: Spectrum showing the noise floor of the HP3047A system with the input mixer powered from the mains (**blue trace**), or with batteries (**red trace**).

To-date, the synchronisation control unit has been situated and operated *locally* within the laser room, utilising the signal derived from a photodiode inside the laser unit and a feed from the RF master clock. We intend to move the unit from the laser room to the photoinjector, thus operating with *remote* synchronisation, as shown in figure 4. The laser beam phase signal will be derived from a diode located immediately below the injector, driven by the 1064 nm low-power timing beam. The RF signal will

be derived from a loop out—coupler in the buncher cavity. It is expected that improvements in synchronisation can be realised in this configuration as both laser & RF phase signals will be derived and compared at the point-of-delivery.

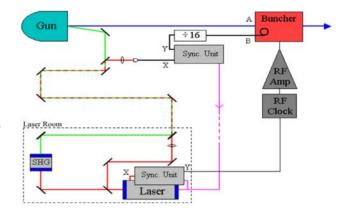


Figure 4: Local and remote synchronisation layouts.

Phase noise measurements show a broad feature caused by relaxation oscillations centred around 300 kHz, though little can be done to reduce its contribution to timing jitter as this is a feature of this particular class of laser. Another feature centred around 800 Hz is caused by inherent limits in the response rate of the feedback loop controlling the mechanical synchronisation hardware. Similarly, little can be done to remove this contribution as any improvements will simply shift the roll–off point to a higher frequency.

The synchronisation unit has not been entirely reliable, having been repaired once already by High Q. The unit has a relatively narrow acquisition range, and the laser must be fully warmed—up before synchronisation can be achieved and maintained reliably. A lack of user–feedback from the unit elevates the High Q engineer's software to a position of great importance, though sadly this utility is not entirely user–friendly itself. These factors may prove a sufficient driver for us to develop our own synchronisation system.

#### REFERENCES

- [1] T. Siggins, C. Sinclair, C. Bohn, D. Bullard, D. Douglas, A. Grippo, J. Gubeli, G.A. Krafft & B. Yunn, "Performance of a DC GaAs photocathode gun for the Jefferson lab FEL", Nuclear Instruments & Methods A; 475 (2001), 549.
- [2] EPICS Experimental Physics and Industrial Control System, Copyright 1991, the Regents of the University of California & the University of Chicago Board of Governors.
- [3] R.P. Scott, C. Langrock & B.H. Kolner, "High-dynamic-range laser amplitude & phase noise measurement techniques", Selected Topics in Quantum Electronics; 7(4), (2001), 641.